Check for updates

Preparation and Characterization of pH-Independent Sustained-Release Tablets Containing Hot Melt Extruded Solid Dispersions of Clarithromycin

Tablets Containing Solid Dispersions of Clarithromycin

Qazi Amir Ijaz[1] · Sumera Latif[2] · Qurat-ul-ain Shoaib[1] · Memoona Rashid[1] · Muhammad Sohail Arshad[3] · Amjad Hussain[1] · Nadeem Irfan Bukhari[1] · Sohail Riaz[4] · Nasir Abbas[1,5] ⓘ

Abstract The limited solubility of clarithromycin (CAM), coupled with low bioavailability and rapid elimination, are major shortcomings, needed to be addressed to achieve optimum therapeutic goals. Therefore, sustained-release (SR) tablets containing solid dispersion (SD) granules of CAM were prepared in this study. Initially, SD granules of CAM were prepared by hot melt extrusion (HME) technique using Kollidon VA64 as a hydrophilic carrier. The saturation solubility of SD showed almost 4.5-fold increase as compared to pure CAM in pH 6.8 medium. *In vitro* drug dissolution data indicated a substantial increase in the dissolution of SD as compared to that of pure CAM. The thermal stability of drug, carrier, and SD at elevated HME temperatures was evident from the results of thermogravimetric analysis (TGA) and differential scanning calorimetry (DSC). Powder X-ray diffraction (PXRD) data and scanning electron microscope (SEM) images revealed a decrease in the crystallinity and the uniform dispersion of drug, respectively. Moreover, Fourier transformed infrared spectroscopy (FT-IR) data confirmed the formation of hydrogen bond between the carbonyl group of drug and the hydroxyl group of carrier. SD loaded sustained-release (SD-SR) matrix tablets were prepared with hydrophobic polymers (Eudragit RS100 and Eudragit RL100). The pH-independent swelling and permeability of both polymers were responsible for the sustained drug release from SD-SR tablets. Pharmacokinetic (PK) studies suggested a 3.4-fold increase in the relative bioavailability of SD-SR tablets as compared to that of pure CAM.

[1] Punjab University College of Pharmacy, University of the Punjab Lahore, Lahore, Pakistan

[2] Institute of Pharmacy, Faculty of Pharmaceutical and Allied Health Sciences, Lahore College for Women University, Lahore, Pakistan

[3] Faculty of Pharmacy, Department of Pharmaceutics, Bahauddin Zakaria University, Multan, Pakistan

[4] Akson College of Pharmacy, Mirpur University of Science & Technology, Mirpur AJ &K, Mirpur, Pakistan

[5] To whom correspondence should be addressed. (e–mail: nasir.pharmacy@pu.edu.pk; nasirabbas77@gmail.com)

Abbreviations
BBD, Box-behnken Design; *BS*, Backscarttering; *CFU*, Colony-Forming unit; *CL_NP*, Cluser of nanoparticles; *Coated_LGG*, Coated *Lacticaseibacillus rhamnous* GG; *CPPs*, Critical process parameters; *CQAs*, Critical quality attributes; *CTRL*, Control; *DLS*, Dynamic light diffusion; *DoE*, Design of the experiment; *EDL*, Electric double layer; *LAB*, Lactic acid bacteria; *LGG*, Lacticaseibacillus rhamnous GG; *MCs*, Micricapsules; *NPs*, Nanoparticles; *PCs*, Photon correlation spectroscopy; *PDI*, Polydispersity index; *QTTP*, Quality target profile; *SD*, Standard deviation; *T*, Transmission; *TEM*, Transmission electron microscopy; *TSI*, Turbiscan Stability Index; *TSS*, Total soluble solids; *ZP*, Zeta potential

INTRODUCTION

The majority of drugs being discovered exhibit poor aqueous solubility and are classified as BCS Class II drugs (1). The limited solubility of class II drugs leads to poor dissolution rate and lower bioavailability (2). One of the most promising methods to enhance the dissolution rate is the delivery of drugs in the form of amorphous solid dispersion by using efficient hydrophilic carriers (3). Carriers including polyethylene glycol, poloxamer, different Eudragit grades, gelucire, and polyvinylpyrrolidone have a propensity to form molecular complexes with a variety of drug substances owing to their strong hydrophilic nature (4). Interaction of hydrophobic drug and hydrophilic carrier can be increased by intense mixing of drug and carrier in the presence of a surfactant using sophisticated

homogenization techniques such as hot melt extrusion (HME) (5). HME is a continuous process in which the powder drug and excipient blend is homogenously mixed by pumping the materials through heated rotating screw (6). HME can offer several advantages over conventional homogenization methods, i.e., (a) atmosphere friendly by eliminating the use of solvent, (b) intensive mixing of the components can facilitate uniform molecular dispersion and conversion of drug into amorphous form resulting in greater solubility and bioavailability (7, 8), and (c) drug release profile can also be modulated by proper selection of polymers (9).

On the other hand, sustain release (SR) dosage systems are known to maintain drug concentration within the effective therapeutic range for drugs having short elimination half-life in plasma over a prolonged time period to achieve desired therapeutic efficacy (10). SR can demonstrate likely advantages over immediate release (IR) dosage forms, i.e., decreased fluctuations in plasma drug concentration, reduced gastrointestinal side effects, ease of administration, and patient compliance. Moreover, SR can effectively achieve optimum therapeutic profile for drugs requiring frequent dosing in chronic diseases (11). SR dosage forms containing poorly water-soluble drugs require both solubilization and release-modulation for better therapeutic efficacy (12, 13). Recently, SR dosage forms containing solid dispersion (SD-SR) have been reported as a promising pharmaceutical approach in an attempt to improve the dissolution and patient compliance concomitantly (14, 15).

Therefore, considering this background, a combination of SD and SR can be proposed. Clarithromycin (CAM) was selected as a model drug for this study because of its shorter elimination half-life (2.6–4.4 h), poor water solubility, and reduced bioavailability (<55%) after oral administration (16, 17). Previously, several attempts have been made to modify the release profile of CAM but still a question remained on its limited solubility (18). Therefore, SD-SR approach could be a better way forward to overcome the above described shortcomings related to CAM. Kollidon VA64 was selected as a carrier owing to its greater hydrophilicity and thermal stability (19). The pH-independent swelling and permeability of Eudragit RS100 and Eudragit RL100 advocated their selection as sustained-release polymers (20).

In this study, we have attempted to prepare hot melt extruded SD in a bid to enhance the dissolution rate and bioavailability of CAM. Then, SD granules were directly compressed into SR tablets to achieve pH-independent sustained-release of the drug. Structural parameters were studied by scanning electron microscope (SEM), Fourier transform infrared spectroscopy (FT-IR), and powder X-ray diffraction (PXRD). Thermal stability of pure drug, carrier, and SD was evaluated by thermogravimetric analysis (TGA) and differential scanning calorimetry (DSC). In addition to *in vitro* drug dissolution, *in vivo* pharmacokinetic (PK) studies were also performed to compare the bioavailability of SD-SR tablets with that of pure drug.

MATERIALS AND METHODS

Materials

CAM was received as a kind gift from Akson Pharmaceuticals, Mirpur, Pakistan. Eudragit RS100 and Eudragit RL100 were purchased from Evonik, Germany. Kollidon VA64, polysorbate 80, and talc were purchased from Sigma Aldrich, USA. HPLC grade acetonitrile was purchased from Tedia, USA. Monobasic potassium phosphate, sodium acetate, hydrochloric acid, acetone, acetic acid, and orthophosphoric acid were purchased from Sitara Chemical Industries, Pakistan.

Preparation of SD *via* HME

A mixture of drug, Kollidon VA64, and polysorbate 80 (50:45:5% w/w/w) was pre-blended in a high shear granulator (BMG, Germany) for 3–5 min at 300 rpm to prepare physical mixture (PM). The PM was then added to the feeding zone of co-rotating Prism 16 mm Twin-screw extruder (Thermo Fisher Scientific, USA), which consisted of a cylindrical-shaped die with 1.75 mm die nozzle, rotated at 50 RPM. The extruder had three heating zones which, from feeding zone to the die, had set points ranging from 120 to 140 °C. After cooling, extrudates were crushed in a shear mill (ESB-500X, Shanghai, China) and pulverized at 20,000 rpm for 5 min. Finally, the powder was sieved through a British Standard Sieve (BSS) of pore size 180 µm.

HPLC Analysis

The quantitative analysis of CAM was performed using HPLC system (1200 series, Agilent Technologies, Germany) equipped with an isocratic pump (G-1310/A), degasser (G-1379/A), column thermostat (G-1316/A), auto sampler (G-1329/A), fluorescent light detector (G-1321/A), diode array detector (DAD) (G-1312/A), and chem station LC/LCMS for windows. Eclipse X DB C18 (5 µm, 4.6 × 250 mm) column was used as a stationary phase to carry out elusion. Monobasic potassium phosphate buffer

(0.035 M) and acetonitrile (68:32 *v/v*), adjusted to pH 4.5 with diluted orthophosphoric acid, was used as an isocratic mobile phase. Twenty microliters of the sample was filtered through a 0.22-μm membrane filter (Minisart, Sartorius, Germany) and eluted at the flow rate of 1 mL min^{-1} through the column maintained at 40 °C temperature and detected by a diode array detector, set at 205 nm. Prior to analysis, HPLC method was validated in terms of linearity, precision, and accuracy. The linearity was attained in concentration range of 10–150 μg/mL ($R = 0.9996$). Inter- and intra-day precision was calculated as % RSD and values were <2%. The accuracy was determined by using three different concentrations of CAM and percentage recovery was in the range of 98–102%.

Characterization of SD

Post-processing Drug Content

HPLC analysis was performed for quantitative determination of CAM in extruded SD. SD granules were dissolved in acetone to achieve a drug concentration of 1 mg/mL and diluted with HPLC mobile phase to a concentration of 100 μg/mL. The amount of drug recovered was stated as total drug present in the SD.

Saturation Solubility

A saturation solubility evaluation was performed in 0.05 M monobasic potassium phosphate buffer solution (pH 6.8) and 0.1 M sodium acetate buffer solution (pH 5.0). An excess quantity of pure CAM, PM, and SD was separately dispersed into 5 mL each of medium in a test tube and mechanically stirred in a water bath for 72 h at a temperature of 37.0 °C. One milliliter of sample was collected at the predetermined times and filtered through a 0.22-μm membrane filter. Fresh medium was added to maintain the volume of the test tube. The filtrate was diluted with HPLC mobile phase to a suitable concentration and then analyzed by HPLC. Three measurements were taken and the mean solubility data was calculated.

Fourier Transform Infrared Spectroscopy

The FT-IR analysis of pure drug, Kollidon VA64, and SD was performed using FT-IR 8400 S, Shimadzu, Japan. Samples were mixed with KBr after size reduction in mortar and pestle and compacted into 6-mm discs with pressure after drying at 40 °C. FTIR spectrum was recorded within 4000–650 cm^{-1}.

Powder X-ray Diffraction

The PXRD analysis of pure drug, Kollidon VA64, and SD was performed using an X-ray diffractometer (JDX-3532, JEOL, Japan) with Cu Kα radiation ($\lambda = 1.54$ Å) having a position-sensitive detector (PSD). Data was collected within $2\theta = 5$–35° keeping the step size 0.02°.

Thermogravimetric Analysis

TGA was performed using a TGA analyzer (Pyris Diamond Series, Perkin-Elmer, USA) using 6.0–7.0 mg of sample in aluminum crucibles surrounded by energetic nitrogen atmosphere. Sample specimen was analyzed by running the experiment at 5 °C/min heating run between temperature range 20 and 500 °C.

Differential Scanning Calorimetry

DSC studies of CAM, Kollidon VA64, and SD was performed using a TA instrument (Q 2000, USA). Approximately 10 mg of sample was placed on an aluminum pan and scanned over a temperature range of 20–350 °C by keeping the heating rate at 10 °C per minute. Nitrogen was used as purged gas flowing at a rate of 50 mL per minute.

The percentage crystallinity was calculated by the DSC method reported by Smith *et al*. ([21]). The formula for calculation of residual crystallinity is given as follows:

$$Xc(\%) = \frac{\Delta H_{m,\alpha}}{\Delta H_{m,\alpha(100\% \text{ crystalline})}} \times 100 \qquad (1)$$

where *Xc* is the estimate for residual crystallinity and $\Delta H_{m,\alpha}$ is the melting endotherm of clarithromycin (J g^{-1}).

Scanning Electron Microscope

The morphology of pure CAM and SD was examined using SEM (JSM-5910, Japan). Scanning was performed with the help of a secondary imaging technique with different magnifications. Analysis was performed under 30 kV accelerating voltage and 63,000 nA emission current.

Preparation of SD-SR Matrix Tablets

SD, hydrophobic polymers, and other excipients were mixed for 5 min and passed through a BSS of pore size 180 μm. SD-SR tablets were prepared by direct compression using 16-mm oval-shaped punch and die set on single punch eccentric tablet press (EP-1, Erweka, Germany) by

Table I Composition of SD-SR Tablets (mg)

Code	SD	Eudragit RS100	Eudragit RL100	Lactose	Talc	Total weight
G1	500	250	0	145	5	900
G2	500	300	0	95	5	900
G3	500	350	0	45	5	900
G4	500	0	350	45	5	900
G5	500	175	175	45	5	900

SD contain drug, Kollidon VA64, and polysorbate 80 (50:45:5% w/w/w) equivalent to 250 mg of drug

applying compression pressure of 12 KN. Composition of different SD-SR tablets is represented in the Table I.

Pharmacotechnical Characterization of the Tablets

Various quality controlled tests such as thickness, hardness, friability, and weight variation were performed and evaluated according to the guidelines given in United States Pharmacopeia (USP). Thickness of the tablets ($n = 10$) was measured using a digital caliper (Mitutoyo, Japan). Mean and standard deviation were evaluated. Hardness of the tablets ($n = 10$) was calculated using a hardness tester (Pharmatron Multitest 50H). Results were reported as kg/cm^2. Mean and standard deviation were evaluated.

For friability studies, weight of ten tablets was calculated and placed in Roche friabilator (Curio, Pakistan) operating at 25 rpm and dropping the test tablets from 6 in. distance to put mechanical stress on tablets. After 4 min, tablets were again weighed to calculate % friability.

$$F = Wi - Wf / Wi \times 100 \qquad (2)$$

where F is friability, Wi is the initial weight, and Wf is the final weight.

Weight Variation and Content Uniformity

Average weight of 20 randomly selected tablets was measured using electronic balance (Sartorius AG, Goettingen, Germany) and then standard deviation of each tablet weight from the mean weight was calculated to find weight variation.

For content uniformity, 20 tablets were taken and crushed; powder weighing equivalent to one tablet was dissolved in 250 mL of acetone and sonicated for 2 h. The sample was diluted with the HPLC mobile phase to a concentration of 100 µg/mL and then analyzed according to the given HPLC method. Content uniformity was expressed as percentage of the labeled claim. Drug content in the range of 90–110% is considered acceptable (22).

Fig. 1 TGA curves of (**A**) pure CAM, (**B**) Kollidon VA64, and (**C**) SD
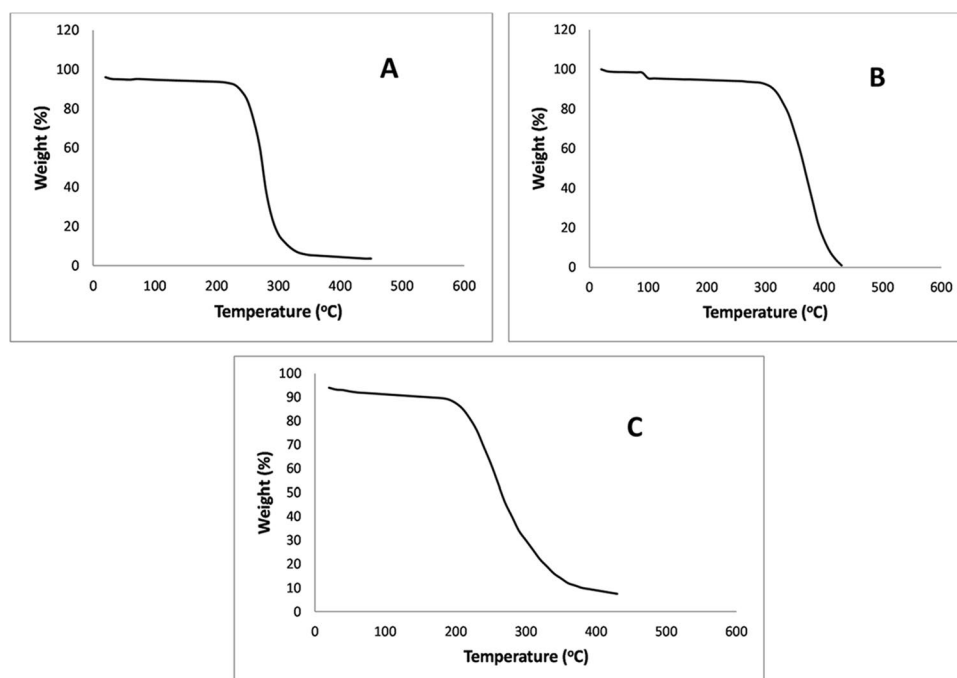
Fig. 2 DSC curves of pure
CAM, Kollidon VA64, PM,
and SD
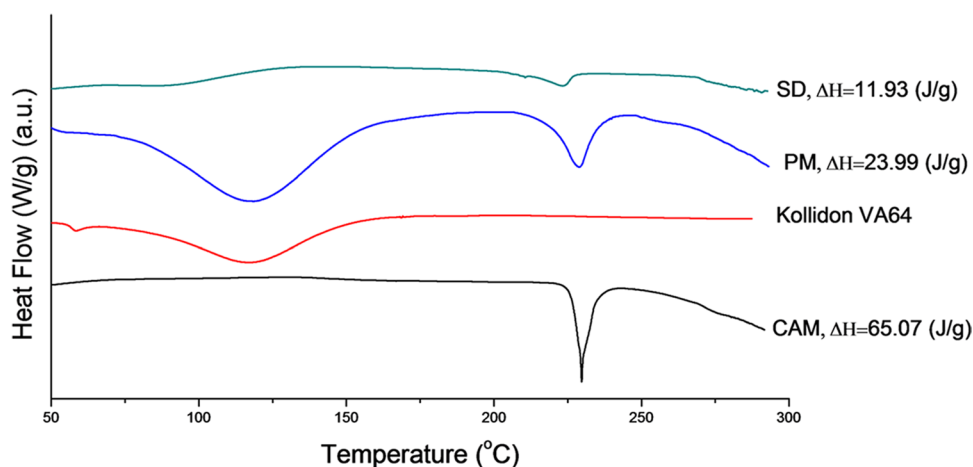
In Vitro Drug Dissolution

In vitro release performance of pure CAM, PM, SD, and SD-SR tablets was evaluated using a United States Pharmacopeia (USP) dissolution apparatus II. The dissolution method developed by Morakul *et al*. was used in this study (22). The dissolution medium (900 mL) was stirred at 50 rpm and temperature was maintained at 37 ± 1 °C. The dissolution study of pure CAM, PM, and SD was performed in 0.05 M monobasic potassium phosphate buffer solution pH 6.8 and 0.1 M sodium acetate buffer solution pH 5.0 for 02 h. While the dissolution study of SD-SR tablets was performed in two phases, initially in 0.1 N HCl for 02 h and then in pH 6.8 buffer solution for 22 h, 1 mL of the sample was withdrawn at 1/6, 1/3, 1/2, 3/4, 1, 2, 3, 4, 6, 8, 10, 12, 16, and 24 h and the same volume of fresh medium was added to the vessels so that the total volume of dissolution medium remained constant. Samples were analyzed according to the HPLC method described previously in the "HPLC

analysis" section. Concentration of drug present in samples was determined from the regression correlation Eq. (23).

Drug release patterns were analyzed according to zero order, first order, Higuchi model, and Korsmeyer-Peppas models. Selection of most appropriate method was established by the value of r^2 close to 1 (24). The release exponent "n" calculated from the Korsmeyer-Peppas model is dependent on the system geometry which governs the release mechanism. When $n = 0.5$, release order is fickian, $n = 1$ is corresponding to case II transport, and $0.5 < n < 1$ is in indicative of non-fickian diffusion mechanism (25).

Pharmacokinetic Studies

A method developed by Amini and Ahmadiani was used for bio-analytical quantification of CAM by RP-HPLC (26). Stock solution was spiked with rabbit plasma to prepare

Fig. 3 FT-IR spectra of pure
CAM, Kollidon VA64, and SD
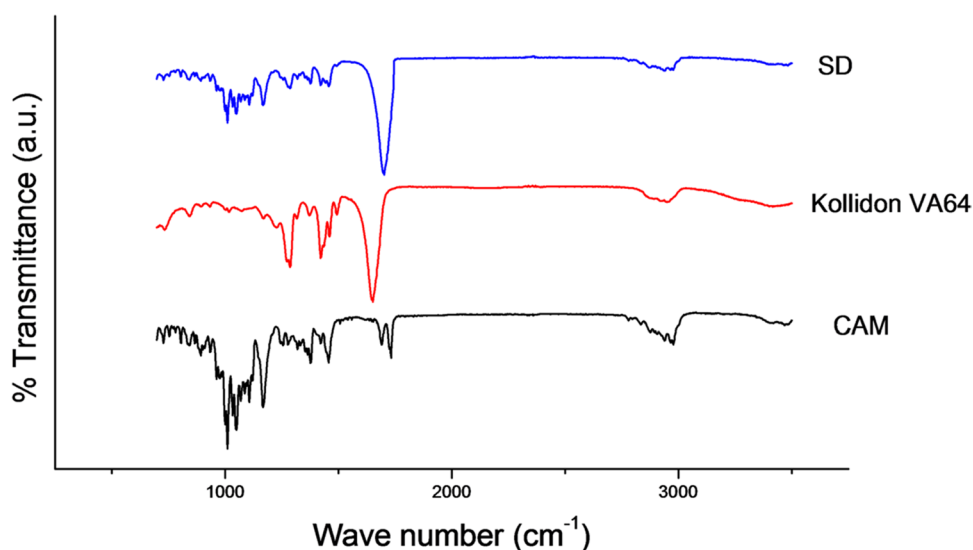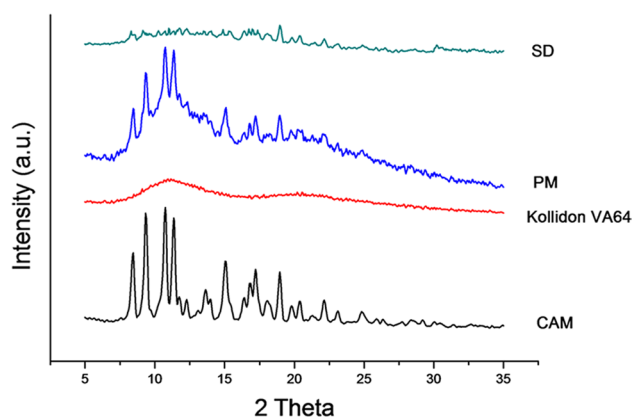
Fig. 4 PXRD spectra of pure CAM, Kollidon VA64, PM, and SD

sample solutions and final concentrations were adjusted to 31.25, 62.5, 125, 250, 500, 1000, and 2000 ng/mL. PK studies were performed using male albino rabbits after oral administration of 40 mg/kg of the drug. This research study involving rabbits was approved by the animal ethical committee of the Punjab University College of Pharmacy, University of the Punjab, Lahore, Pakistan (AEC/PUCP/1106).

Eighteen healthy male rabbits were selected and placed in the animal house. Six rabbits were given the pure CAM, other six were given SD, and the rests were given the SD-SR tablets after overnight fasting to minimize the effect of food on drug absorption. Blood samples were obtained from the marginal ear vein of the rabbits at pre-determined time intervals of 1/2, 1, 2, 4, 6, 8, 10, 12, 16, and 24 h. The samples were centrifuged at 10,000 g for 5 min to extract plasma and plasma layer was transferred to 4 mL polypropylene tube. In order to perform extraction, 1 mL of plasma was vortex mixed with 20 µL of 1 M NaOH and 2.5 mL of n-hexane/1-butanol (98:2, v/v) in a polypropylene tube. After 3-min centrifugation at 12,000 g, whole organic layer was separated and transferred to another tube. Then, 50 µL of 0.1% acetic acid was added and vortex mixed for 5 min. After that, the mixture was centrifuged at 12,000 g for 2 min. After

discarding upper organic phase, the aqueous phase was used for HPLC analysis according to the chromatographic conditions described previously in the "HPLC analysis" section. PK parameters were calculated using PK solver version 2.0 (27).

Statistical analysis was performed using SPSS 17. One-way analysis of variance (ANOVA) was used to compare PK parameters and statistical significance was defined at $p < 0.05$.

RESULTS AND DISCUSSION

Preparation and Characterization of SD

It is important to consider the thermal properties of the drug and excipients before the process of HME in order to avoid the drug degradation (28). Therefore, TGA and DSC of pure CAM, Kollidon VA64, and SD were performed and results are illustrated in Fig. 1 and Fig. 2. The TGA curve of pure CAM showed a major thermal event at around 230 °C, caused by the degradation of drug. Greater thermal stability of Kollidon VA64 was evident from its thermal behavior, as it started to degrade at about 350 °C. The TGA curve of SD showed slight shifting of thermal events towards lower temperatures, and this behavior was likely to be caused by the changes in crystalline properties of the drug after extrusion. The DSC thermogram of pure CAM (Fig. 2) displayed an endothermic peak at 229 °C corresponding to the melting point of the drug. This sharp peak indicated that the pure CAM was in crystalline form (29). A broad endothermic peak at 80–120 °C is visible in the thermogram of Kollidon VA64, which can be attributed to the loss of water content. The sharp endothermic peak of the drug disappeared in the SD thermogram, which is indicative of a decrease in the crystallinity of drug (30). The post-HME drug content of SD was determined by HPLC quantitative analysis and was found to be 98.4 ± 2.3%. The residual crystallinity calculated was 36.87% and 18.33% for PM and SD, respectively. The

Fig. 5 SEM images of **A** pure CAM and **B** SD
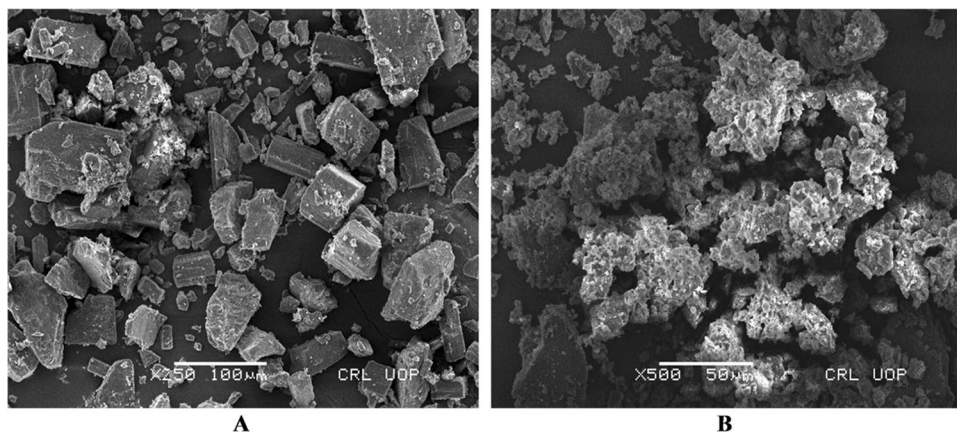
Table II Summary of Physical Properties of SD-SR Tablets ($n=3$)

| Formulation	Thickness (mm)	Hardness (kg/cm^2)	Friability (%)	Weight variation (mg)	Content uniformity (%)
G1	3.16 ± 0.12	6.32 ± 0.21	0.45 ± 0.023	895 ± 11.52	98.12 ± 1.12
G2	3.21 ± 0.11	6.83 ± 0.25	0.44 ± 0.021	897 ± 15.68	99.76 ± 1.43
G3	3.32 ± 0.09	6.93 ± 0.31	0.31 ± 0.078	905 ± 16.12	98.89 ± 2.21
G4	3.28 ± 0.08	6.81 ± 0.34	0.35 ± 0.083	907 ± 11.31	99.42 ± 1.31
G5	3.24 ± 0.15	6.74 ± 0.28	0.48 ± 0.041	903 ± 09.62	98.82 ± 1.08

presence of small number of crystals of drug may accelerate the recrystallization process. For this reason, a crystallization inhibitor (Kollidon VA 64) was added which interact with the drug molecules and inhibit and/or retards the re-crystallization.

It is pertinent to note that a decrease in crystallinity of drug is achieved, but it was difficult to attain complete amorphization at these experimental conditions. This may be due to lack of mixture homogeneity (large bulk) and less contact time in melting chamber. One may achieve complete amorphization of the drug at higher polymeric fractions and/or employing protracted thermal exposures. Nevertheless, processing conditions related thermal degradation of drug increase gross weight of the individual doses which may push the study beyond operational limits.

FT-IR analysis was performed to observe the drug-polymer interactions usually resulting in peak shifting or absence/appearance of absorption peaks. The FT-IR spectrum of pure CAM (Fig. 3) displayed the representative band of hydrogen bonds between -OH groups vibration at 3466 cm^{-1}, –O– ether function bands at 1090 cm^{-1}, O–C=O stretching vibration in lactone ring at 1733 cm^{-1}, N-CH3 stretching of aromatic ring at 1424 cm^{-1}, and alkyl-CH3 substitution bands at 2940 cm^{-1} (31). The FT-IR spectrum of Kollidon VA64 presented peaks for carbonyl stretching at 1650 cm^{-1} and C-N vibration at 1290 cm^{-1} (32). The FT-IR spectrum of SD displayed all the characteristic peaks of drug and polymers, but slight shifting of carbonyl stretching peak at a higher wavenumber was suggestive of a hydrogen bond formation between the carbonyl group of CAM and the hydroxyl group of Kollidon VA64 after dispersion. This result is in agreement with the study carried out by Watanabe *et al.*, where hydrogen bonding between indomethacin and the carrier was observed (33). The hydrogen bond formation

Fig. 6 **a** Percentage drug dissolved of (A) pure CAM, PM, and SD at pH 6.8; (B) pure CAM, PM, and SD at pH 5 ($n=3$). **b** Percentage drug dissolved of SD-SR tablets ($n=3$)
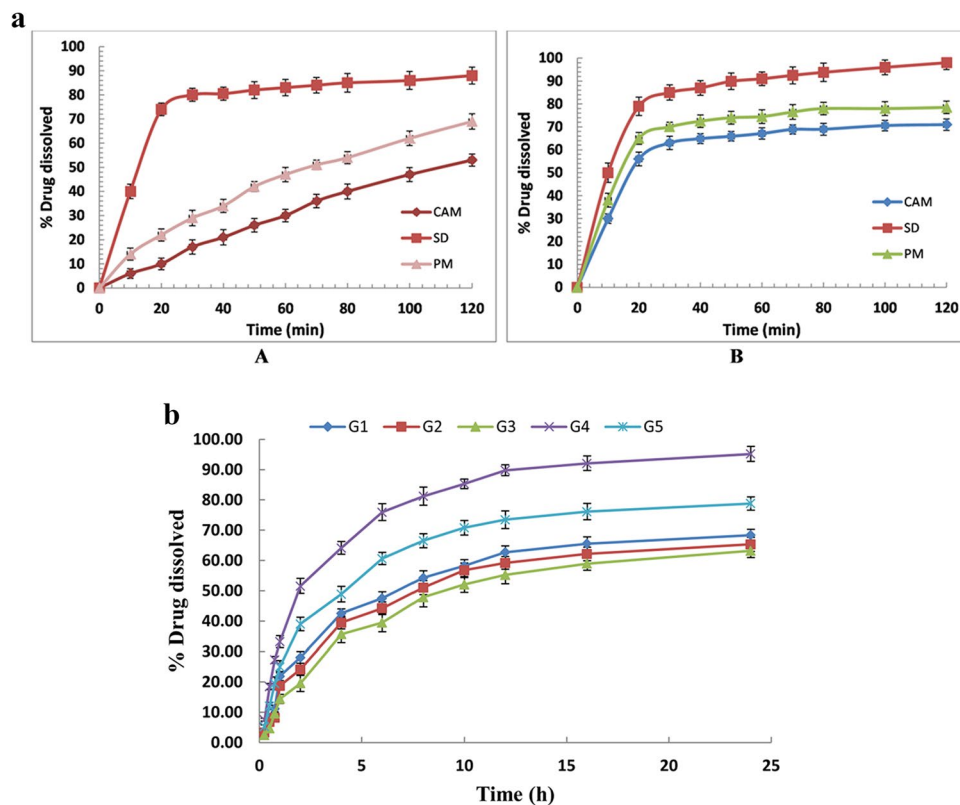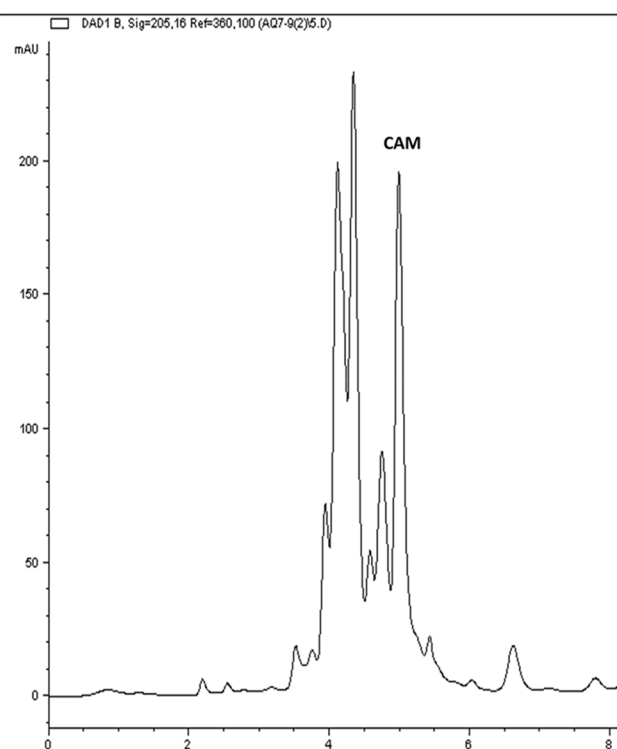
Fig. 7 HPLC chromatogram of CAM in plasma sample after oral administration of SD-SR tablet to rabbits

between Kollidon VA 64 (carrier) and drug is considered to play a vital role in preventing recrystallization of amorphous drugs. The inclusion of carrier might inhibit the association of the drug molecule to form the crystal nucleus and inhibit the crystal growth (34).

PXRD was conducted to study the physical state of pure drug and SD granules. The PXRD pattern of pure CAM (Fig. 4) demonstrated the crystalline nature of drug owing to the presence of several distinctive peaks as consistent with literature (35). No distinctive peak of Kollidon VA64 was observed, thus confirming its amorphous nature (36). A decrease in the crystalline behavior of the drug was evident from the PXRD pattern of SD, as intensity of all the distinctive peaks showed a decline. Similar type of behavior was observed previously by Tantishaiyakul et al. (37).

SEM images of pure CAM and SD are depicted in Fig. 5. SEM images of pure CAM showed small and large crystals of the drug. On the other hand, SEM images of SD displayed uniformly dispersed drug particles with enhanced surface area, which is important for a representative dissolution and bioavailability in drug delivery. These results are not unusual as similar outcomes were observed earlier by Fini et al. (38).

An increase in the saturation solubility is one of the characteristic features of SD (39). CAM shows pH-dependent solubility as it is a weakly basic drug with a pKa of 8.8. Therefore, greater solubility of CAM was observed at pH 5 as compared to pH 6.8. The saturation solubility of pure CAM, PM, and SD as studied in different media evidenced the solubility enhancement of CAM after dispersion. The saturation solubility of pure CAM, PM, and SD in 6.8 pH buffer solution was 0.62 ± 0.15 mg/mL, 0.94 ± 0.23 mg/mL, and 2.96 ± 0.21 mg/mL, respectively. These results revealed almost 1.5 times increase in the solubility of PM and 4.5 times increase in solubility of the SD as compared to pure CAM. The saturation solubility of pure CAM, PM, and SD in pH 5.0 buffer medium was 2.82 ± 0.28 mg/mL, 3.97 ± 0.37 mg/mL, and 8.23 ± 0.43 mg/mL, respectively, thus, indicating nearly 1.4 times increase in the solubility of PM and 3 times increase in the solubility of SD as compared to pure CAM. This enhanced solubility of PM as compared to pure CAM in aqueous solutions can be credited to the improved wetting and miscibility caused by the hydrophilic nature of polysorbate 80 (40). Comparable outcomes were observed by Peng et al., when saturation solubility of lopinavir was increased using polymeric surfactants (41). The improvement in solubility of SD as compared to pure CAM can be attributed to the dispersion of drug in amorphous form (Fig. 4) and intermolecular interactions between drug and hydrophilic carrier (Fig. 3).

Pharmacotechnical Characterization of the Tablets

All the formulations were observed to abide the USP limits of thickness, hardness, friability, weight variation, and content uniformity (Table II). Hardness of tablets was in the range of 6.32 ± 0.21–6.93 ± 0.31 kg/cm^2, while thickness of the all the tablets was in the range of 3.16 ± 0.12–3.32 ± 0.09 mm. Friability result of all the

Table III Release Kinetics of Different SD-SR Tablets	Sample code	Zero-order kinetics		First-order kinetics		Higuchi model		Korsmeyer-Peppas model		
		K_o	r^2	K_1	r^2	K_2	r^2	K_3	r^2	n
	G1	0.0418	0.756	0.0892	0.849	0.1694	0.924	0.0961	0.871	0.616
	G2	0.0396	0.772	0.0783	0.854	0.1532	0.933	0.0854	0.883	0.640
	G3	0.0373	0.799	0.0681	0.877	0.1491	0.949	0.0727	0.910	0.671
	G4	0.0603	0.699	0.2752	0.938	0.2426	0.911	0.1668	0.876	0.552
	G5	0.0494	0.721	0.1398	0.842	0.1814	0.918	0.1281	0.892	0.581

Table IV Pharmacokinetic Parameters of Pure CAM, SD, and SD-SR ($n=6$)

Parameters	Unit	Pure CAM Mean±SD	SD Mean±SD	SD-SR Mean±SD
Cmax	ng/mL	1166.54±254.12	2042.17±468.43**	1540.00±377.12**
Tmax	h	3.89±0.16	2.00±0.20*	6.20±0.40**
t1/2	h	6.17±0.25	4.23±0.36*	11.69±0.58**
AUC 0-inf	ng/mL*h	8858.25±544.11	12,219.88±684.29**	30,241.12±822.14**
AUMC 0-inf	ng/mL*h^2	68,474.42±843.57	57,983.26±871.16*	596,205.98±4078.18**
MRT 0-inf	h	7.73±0.87	4.74±0.59*	19.71±1.44**
R.B	%age	–	138**	341**

*Significantly lower than pure CAM ($p < 0.05$)

**Significantly higher than pure CAM ($p < 0.05$)

studied formulations was observed to be within the limits given in USP (<1%). Weight variation of all the tablets was <5%, thus meeting the official pharmacopeia requirements for weight variation. Results of content uniformity indicated percentage content of active substance in all the formulations lying within the USP limits (90–110%). Based on the results, it can be inferred that CAM SD-SR tablets with optimum physicochemical properties can be prepared by direct compression.

In Vitro Drug Dissolution

In vitro drug release performance of pure CAM, PM, and SD was studied in pH 5 and 6.8 dissolution medium for 02 h (Fig. 6a). Due to its pH dependent solubility, dissolution profile of the drug was greater in pH 5 as compared to pH 6.8 medium. A considerable increase in the dissolution rate of SD was observed as compared to that of pure CAM. On the other hand, the dissolution profile of SD-SR tablets showed sustained drug release for up to 24 h without any burst release (Fig. 6b). This pH-independent release of drug is understandable, as both of the polymers used are

insoluble in aqueous medium, but still permeable due to the presence of quaternary ammonium groups in their structure. Comparable behavior was observed earlier by Pietrzak *et al.* (42). Incremental concentration of Eudragit RS100 demonstrated sustained drug release; i.e., formulation "G3" having a maximum concentration of Eudragit RS100 showed minimum drug release (63.20±2.33%), as compared to other formulations (G1=68.36±1.92%, G2=65.32±3.12%). This observation can be attributed to the fact that an increase in the concentration of Eudragit RS100 leads to a denser and tightly packed structure, making it difficult for the drug particles to migrate in the surrounding medium (43). It was evident from the results that the drug release augmented considerably by replacing Eudragit RS100 with Eudragit RL100; i.e., the formulation "G4" showed the greatest drug release (95.18±2.53%) as compared to all other formulations. This characteristic is vindicated by the presence of excessive quaternary ammonium groups in Eudragit RL100 as compared to Eudragit RS100. The formulation "G5" prepared with a combination of Eudragit RS100 and Eudragit RL100 (50:50) also demonstrated greater drug release (78.81±2.28%) as compared to all the formulations prepared solely with Eudragit RS100. These findings are comparable to the study carried out by Reddy *et al.*, where the drug release of nicorandil was prolonged with the help of Eudragit RS100 and Eudragit RL100 (44).

Drug release kinetics of SR tablets was studied by fitting the *in vitro* drug release data into various models. Values of regression co-efficient (r^2) were considered to determine the goodness of fit of release profile against different models, as given in Table III. The k model showed greatest values of r^2 as compared to all other models, thus indicating the behavior of drug release kinetics in accordance with Higuchi model. Values of release exponent (n) calculated from the Korsmeyer-Peppas model were greater than 0.5 but less than 1 for all the SR formulations, which confirmed the non-fickian diffusion release of the drug.
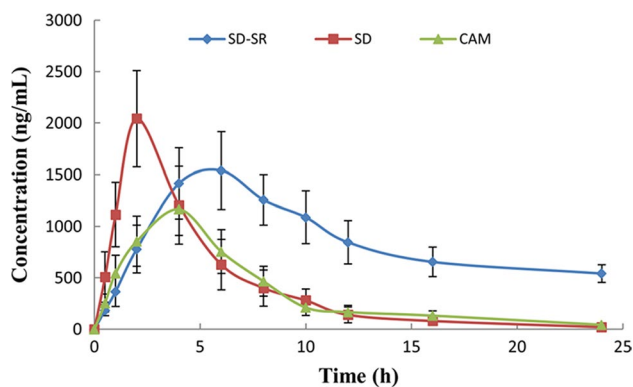
Fig. 8 Plasma level time curves after oral dosing of pure CAM, SD and SD-SR in rabbits (n=6)

Pharmacokinetic Studies

PK studies were performed to compare the relative bioavailability of SD granules and SD-SR tablets with that of pure CAM. Chromatograms of CAM in the plasma sample after oral administration of the drug are illustrated in Fig. 7. PK parameters of pure CAM, SD, and SD-SR tablets are given in Table IV. For pure CAM and SD, a maximum plasma concentration (Cmax) of 1166.54 ± 254.12 and 2042.17 ± 468.43 ng/mL was achieved at 3.89 ± 0.16 and 2.0 ± 0.20 h, respectively, while Cmax (1540.00 ± 377.12 ng/mL) for SD-SR tablets, where drug release was attained in a sustainable fashion, was achieved at 6.20 ± 0.40 h. The half-life (t1/2) of SD-SR tablets (11.69 ± 0.58 h) was significantly greater than that of pure CAM (6.17 ± 0.25 h) and SD (4.23 ± 0.36 h). SD-SR tablets showed greater *in vivo* mean residence time (19.71 ± 1.44 h) as compared to SD (4.74 ± 0.59 h) and pure CAM (7.73 ± 0.87 h). The relative bioavailability of SD was almost 1.4-fold greater as compared to that of pure CAM, while the relative bioavailability of SD-SR tablets was almost 3.4-fold greater as compared to that of pure CAM. The AUC0-inf ($30,241.12 \pm 822.14$ ng/mL*h) of SD-SR tablets was significantly greater than that of pure CAM (8858.25 ± 544.11 ng/mL*h). Sustained drug absorption was evident from the plasma level time curve of SD-SR tablets (Fig. 8). The plasma level time curve of SD-SR tablets exhibited minimum fluctuation in plasma concentration and greater tmax, as compared to those of pure CAM and SD.

CONCLUSION

In this study, SD-SR matrix tablets were prepared in an attempt to increase the solubility and bioavailability of CAM. PK studies reflected a significant increase in the relative bioavailability of SD-SR tablets as compared to that of pure CAM. Different possible mechanisms contributed towards the enhanced solubility and bioavailability of SD-SR: (1) uniform drug dispersion during the process of HME, (2) decrease in the crystallinity of drug, (3) improved wetting and miscibility of the drug caused by hydrophilic carrier and surfactant, (4) intermolecular interactions between drug and carrier, (5) sustained drug absorption for a prolonged period of time. Although the major objective of the study has been achieved, the study focusing on investigation of the impact of the material attributes and hot melt extrusion process parameters on the critical quality attributes of solid dispersions to achieve complete amorphization would be an important future prospect.

Declarations

Conflict of Interest   The authors declare no competing interests.

Supplementary Information   Supplementary information can be provided on demand.

References

1. Shi N-Q, Wang S-R, Zhang Y, Huo J-S, Wang L-N, Cai J-H, *et al*. Hot melt extrusion technology for improved dissolution, solubility and "spring-parachute" processes of amorphous self-micellizing solid dispersions containing BCS II drugs indomethacin and fenofibrate: profiles and mechanisms. Eur J Pharm Sci. 2019;130:78–90. https://doi.org/10.1016/j.ejps.2019.01.019.

2. Borba PAA, Pinotti M, de Campos CEM, Pezzini BR, Stulzer HK. Sodium alginate as a potential carrier in solid dispersion formulations to enhance dissolution rate and apparent water solubility of BCS II drugs. Carbohydr polym. 2016;137:350–9. https://doi.org/10.1016/j.carbpol.2015.10.070.

3. Albadarin AB, Potter CB, Davis MT, Iqbal J, Korde S, Pagire S, *et al*. Development of stability-enhanced ternary solid dispersions via combinations of HPMCP and Soluplus® processed by hot melt extrusion. Int J Pharm. 2017;532:603–11. https://doi.org/10.1016/j.ijpharm.2017.09.035.

4. Zhang X, Xing H, Zhao Y, Ma Z. Pharmaceutical dispersion techniques for dissolution and bioavailability enhancement of poorly water-soluble drugs. Pharmaceutics. 2018;10:74. https://doi.org/10.3390/pharmaceutics10030074.

5. Sotthivirat S, McKelvey C, Moser J, Rege B, Xu W, Zhang D. Development of amorphous solid dispersion formulations of a poorly water-soluble drug, MK-0364. Int J Pharm. 2013;452:73–81. https://doi.org/10.1016/j.ijpharm.2013.04.037.

6. Hörmann T, Jäger N, Funke A, Mürb R-K, Khinast JG, Paudel A. Formulation performance and processability window for manufacturing a dual-polymer amorphous solid dispersion via hot-melt extrusion and strand pelletization. Int J Pharm. 2018;553:408–21. https://doi.org/10.1016/j.ijpharm.2018.10.035.

7. Tran PH, Lee B-J, Tran TT. Recent studies on the processes and formulation impacts in the development of solid dispersions by hot-melt extrusion. Eur J Pharm Biopharm. 2021. https://doi.org/10.1016/j.ejpb.2021.04.009.

8. Hwang I, Kang C-Y, Park J-B. Advances in hot-melt extrusion technology toward pharmaceutical objectives. J Pharm Investig. 2017;47:123–32. https://doi.org/10.1007/s40005-017-0309-9.

9. Ren Y, Mei L, Zhou L, Guo G. Recent perspectives in hot melt extrusion-based polymeric formulations for drug delivery: applications and innovations. AAPS PharmSciTech. 2019;20:1–12. https://doi.org/10.1208/s12249-019-1300-8.

10. Van Snick B, Holman J, Cunningham C, Kumar A, Vercruysse J, De Beer T, *et al*. Continuous direct compression as manufacturing platform for sustained release tablets. Int J Pharm. 2017;519:390–407. https://doi.org/10.1016/j.ijpharm.2017.01.010.

11. Krkobabić M, Medarević D, Cvijić S, Grujić B, Ibrić S. Hydrophilic excipients in digital light processing (DLP) printing of sustained release tablets: impact on internal structure and drug dissolution rate. Int J Pharm. 2019;572: 118790. https://doi.org/10.1016/j.ijpharm.2019.118790.

12. Yi HG, Chi MH, Kim Y-I, Woo JS, Park E-S. Formulation of a extended release tablet containing dexibuprofen. Arch Pharm Res. 2008;31:1637. https://doi.org/10.1007/s12272-001-2162-6.

13. Tran TT-D, Tran PH-L, Lim J, Park JB, Choi S-K, Lee B-J. Physicochemical principles of controlled release solid dispersion containing a poorly water-soluble drug. Ther Deliv. 2010;1:51–62. https://doi.org/10.4155/tde.10.3.

14. Sahoo J, Murthy P, Biswal S. Formulation of sustained-release dosage form of verapamil hydrochloride by solid dispersion technique using eudragit RLPO or Kollidon® SR. AAPS PharmSciTech. 2009;10:27–33. https://doi.org/10.1208/s12249-008-9175-0.

15. Tran HTT, Park JB, Hong K-H, Choi H-G, Han H-K, Lee J, et al. Preparation and characterization of pH-independent sustained release tablet containing solid dispersion granules of a poorly water-soluble drug. Int J Pharm. 2011;415:83–8. https://doi.org/10.1016/j.ijpharm.2011.05.052.

16. Chu S, Deaton R, Cavanaugh J. Absolute bioavailability of clarithromycin after oral administration in humans. Antimicrob Agents Chemother. 1992;36:1147. https://doi.org/10.1128/aac.36.5.1147.

17. Suwa T, Yoshida H, Kohno Y, Yoshitumi S, Ohta K. Metabolic fate of TE-031 (A-56268). III. Absorption, distribution and excretion of 14 C-TE-0341 in rats, mice and dogs. Chemotherapy. 1988;36:213–26. https://doi.org/10.1128/aac.33.5.751.

18. Nama M, Gonugunta CSR, Veerareddy PR. Formulation and evaluation of gastroretentive dosage forms of clarithromycin. AAPS PharmSciTech. 2008;9:231. https://doi.org/10.1208/s12249-008-9038-8.

19. Szafraniec-Szczęsny J, Antosik-Rogóż A, Kurek M, Gawlak K, Górska A, Peralta S, et al. How does the addition of Kollidon® VA64 inhibit the recrystallization and improve ezetimibe dissolution from amorphous solid dispersions? Pharmaceutics. 2021;13:147. https://doi.org/10.3390/pharmaceutics13020147.

20. Das S, Das N. Preparation and in vitro dissolution profile of dual polymer (Eudragit RS100 and RL100) microparticles of diltiazem hydrochloride. J Microencapsul. 1998;15:445–52. https://doi.org/10.3109/02652049809006871.

21. Smith G, Hussain A, Bukhari NI, Ermolina I. Quantification of residual crystallinity in ball milled commercially sourced lactose monohydrate by thermo-analytical techniques and terahertz spectroscopy. Eur J Pharm Biopharm. 2015;92:180–91. https://doi.org/10.1016/j.ejpb.2015.02.026.

22. Goodwin DJ, van den Ban S, Denham M, Barylski I. Real time release testing of tablet content and content uniformity. Int J Pharm. 2018;537:183–92. https://doi.org/10.1016/j.ijpharm.2017.12.011.

23. Blanco M, Coello J, Gonzalez F, Iturriaga H, Maspoch S, Tomas X. Spectrophotometric determination of pharmaceutical dosages by partial least-squares calibration. J Pharm Biomed Anal. 1994;12:509–14. https://doi.org/10.1016/0731-7085(93)e0004-7.

24. Zhang J, Yang W, Vo AQ, Feng X, Ye X, Kim DW, et al. Hydroxypropyl methylcellulose-based controlled release dosage by melt extrusion and 3D printing: Structure and drug release correlation. Carbohydr polym. 2017;177:49–57. https://doi.org/10.1016/j.carbpol.2017.08.058.

25. Ritger PL, Peppas NA. A simple equation for description of solute release II. Fickian and anomalous release from swellable devices. J Control Release. 1987;5:37–42. https://doi.org/10.1016/0168-3659(87)90034-4.

26. Amini H, Ahmadiani A. Sensitive determination of clarithromycin in human plasma by high-performance liquid chromatography with spectrophotometric detection. J Chromatogr B.

2005;817:193–7. https://doi.org/10.1016/j.jchromb.2004.12.003.

27. Zhang Y, Huo M, Zhou J, Xie S. PKSolver: an add-in program for pharmacokinetic and pharmacodynamic data analysis in Microsoft Excel. Comput Methods Programs Biomed. 2010;99:306–14. https://doi.org/10.1016/j.cmpb.2010.01.007.

28. Sarode AL, Sandhu H, Shah N, Malick W, Zia H. Hot melt extrusion (HME) for amorphous solid dispersions: predictive tools for processing and impact of drug–polymer interactions on supersaturation. Eur J Pharm Sci. 2013;48:371–84. https://doi.org/10.1016/j.ejps.2012.12.012.

29. El Nashar NF, Donia AA, Mady OY, El Maghraby GM. Formulation of clarithromycin floating microspheres for eradication of Helicobacter pylori. J Drug Del Sci Techn. 2017;41:213–21. https://doi.org/10.1016/j.jddst.2017.07.016.

30. de Souza CMP, dos Santos JAB, do Nascimento AL, Júnior JVC, Júnior FJdLR, de Lima Neto SA, et al. Thermal analysis study of solid dispersions hydrochlorothiazide. J Therm Anal Calorim. 2018;131:681–9. https://doi.org/10.1007/s10973-017-6091-0.

31. Malladi M, Jukanti R. Formulation development and evaluation of a novel bi-dependent clarithromycin gastroretentive drug delivery system using Box-Behnken design. J Drug Del Sci Techn. 2016;35:134–45. https://doi.org/10.1016/j.jddst.2016.06.003.

32. Vojinović T, Medarević D, Vranić E, Potpara Z, Krstić M, Djuriš J, et al. Development of ternary solid dispersions with hydrophilic polymer and surface adsorbent for improving dissolution rate of carbamazepine. Saudi pharm j. 2018;26:725–32. https://doi.org/10.1016/j.jsps.2018.02.017.

33. Watanabe T, Hasegawa S, Wakiyama N, Kusai A, Senna M. Comparison between polyvinylpyrrolidone and silica nanoparticles as carriers for indomethacin in a solid state dispersion. Int J Pharm. 2003;250:283–6. https://doi.org/10.1016/s0378-5173(02)00549-5.

34. Taylor LS, Zografi G. Spectroscopic characterization of interactions between PVP and indomethacin in amorphous molecular dispersions. Pharm Res. 1997;14:1691–8.

35. Soisuwan S, Teeranachaideekul V, Wongrakpanich A, Langguth P, Junyaprasert VB. Impact of uncharged and charged stabilizers on in vitro drug performances of clarithromycin nanocrystals. Eur J Pharm Biopharm. 2019;137:68–76. https://doi.org/10.1016/j.ejpb.2019.02.004.

36. Jijun F, Lishuang X, Xiaoguang T, Min S, Mingming Z, Haibing H, et al. The inhibition effect of high storage temperature on the recrystallization rate during dissolution of nimodipine–Kollidon VA64 solid dispersions (NM–SD) prepared by hot-melt extrusion. J Pharm Sci. 2011;100:1643–7. https://doi.org/10.1002/jps.22429.

37. Tantishaiyakul V, Kaewnopparat N, Ingkatawornwong S. Properties of solid dispersions of piroxicam in polyvinylpyrrolidone. Int J Pharm. 1999;181:143–51. https://doi.org/10.1016/s0378-5173(99)00070-8.

38. Fini A, Moyano JR, Ginés JM, Perez-Martinez JI, Rabasco AM. Diclofenac salts, II. Solid dispersions in PEG6000 and Gelucire 50/13. Eur J Pharm Biopharm. 2005;60:99–111. https://doi.org/10.1016/j.ejpb.2004.11.005.

39. Pawar J, Tayade A, Gangurde A, Moravkar K, Amin P. Solubility and dissolution enhancement of efavirenz hot melt extruded amorphous solid dispersions using combination of polymeric blends: a QbD approach. Eur J Pharm Sci. 2016;88:37–49. https://doi.org/10.1016/j.ejps.2016.04.001.

40. Okonogi S, Puttipipatkhachorn S. Dissolution improvement of high drug-loaded solid dispersion. AAPS PharmSciTech. 2006;7:E148–53. https://doi.org/10.1208/pt070252.

41. Zi P, Zhang C, Ju C, Su Z, Bao Y, Gao J, et al. Solubility and bioavailability enhancement study of lopinavir solid dispersion

matrixed with a polymeric surfactant-Soluplus. Eur J Pharm Sci. 2019;134:233–45. https://doi.org/10.1016/j.ejps.2019.04.022.

42. Pietrzak K, Isreb A, Alhnan MA. A flexible-dose dispenser for immediate and extended release 3D printed tablets. Eur J Pharm Biopharm. 2015;96:380–7. https://doi.org/10.1016/j.ejpb.2015.07.027.

43. Nath B, Nath LK, Kumar P. Preparation and in vitro dissolution profile of zidovudine loaded microspheres made of Eudragit RS 100, RL 100 and their combinations. Acta Pol Pharm. 2011;68:409–15. https://doi.org/10.4314/jophas.v7i3.63406.

44. Reddy KR, Mutalik S, Reddy S. Once-daily sustained-release matrix tablets of nicorandil: formulation and in vitro evaluation. AAPS PharmSciTech. 2003;4:480–8. https://doi.org/10.1208/pt040461.